

Transfer Learning for Classification of Cardiovascular Tissues in Histological Images

Claudia Mazo^{a,1,*}, Jose Bernal^{b,1}, Maria Trujillo^c, Enrique Alegre^d

^a*University College Dublin, CeADAR: Centre for Applied Data Analytics Research, School of Computer Science, Dublin, Ireland*

^b*Universitat de Girona, Institute of Computer Vision and Robotics, Girona, Spain*

^c*Universidad del Valle, Computer and Systems Engineering School, Cali, Colombia*

^d*Universidad de León, Industrial and Informatics Engineering School, León, Spain*

Abstract

Background and Objective: Automatic classification of healthy tissues and organs based on histology images is an open problem, mainly due to the lack of automated tools. Solutions in this regard have potential in educational medicine and medical practices. Some preliminary advances have been made using image processing techniques and classical supervised learning. Due to the breakthrough performance of deep learning in various areas, we present an approach to recognise and classify, automatically, fundamental tissues and organs using Convolutional Neural Networks (CNN).

Methods: We adapt four popular CNNs architectures – ResNet, VGG19, VGG16 and Inception – to this problem through transfer learning. The resulting models are evaluated at three stages. Firstly, all the transferred networks are compared to each other. Secondly, the best resulting fine-tuned model is compared to an ad-hoc 2D multi-path model to outline the importance of transfer learning. Thirdly, the same model is evaluated against the state-of-the-art method, a cascade SVM using LBP-based descriptors, to contrast a traditional machine learning approach and a representation learning one. The evaluation task consists of separating six classes accurately: smooth muscle of the elastic

*Corresponding author

Email address: claudia.mazovargas@ucd.ie (Claudia Mazo)

¹These authors contributed equally to this work

artery, smooth muscle of the large vein, smooth muscle of the muscular artery, cardiac muscle, loose connective tissue, and light regions. The different networks are tuned on 6000 blocks of 100×100 pixels and tested on 7500.

Results: Our proposal yields F-score values between 0.717 and 0.928. The highest and lowest performances are for cardiac muscle and smooth muscle of the large vein, respectively. The main issue leading to limited classification scores for the latter class is its similarity with the elastic artery. However, this confusion is evidenced during manual annotation as well. Our algorithm reached improvements in F-score between 0.080 and 0.220 compared to the state-of-the-art machine learning approach.

Conclusions: We conclude that it is possible to classify healthy cardiovascular tissues and organs automatically using CNNs and that deep learning holds great promise to improve tissue and organs classification. We left our training and test sets, models and source code publicly available to the research community.

Keywords: Transfer learning, SVM, fundamental tissues, organs, cardiovascular system, histological images

1. Introduction

The recognition of normal fundamental tissues and organs is predominantly carried out by histology experts or similar. Only a few systems can recognise fundamental tissues and organs automatically [1, 2, 3]. However, the accuracy of
5 these tools is not yet comparable to human raters, i.e. this task is still an open problem. Automatic classification of tissues and organs in histological images of the human cardiovascular system has potential in educational medicine [4] as it could increase the number of cases that a student could analyse – promoting self-learning [5] – and facilitate online learning to external or remote experts and
10 students. These types of solutions require lower social and economic investment than traditional strategies for obtaining well-trained professionals. Besides, automatic classification enables labelling of large repositories available in different

hospitals. Consequently, issues associated with manual classification (e.g. subjectivity, time, difficulty, costs, and impracticality) could be mitigated [6].

15 The computer-aided recognition of normal and pathological fundamental tissues and organs has been addressed using different features and techniques. Engineered characteristics related to colour, texture and shape have been used within image processing pipelines for describing [7, 8, 9, 10, 11] and recognising fundamental tissues [12, 13]. Convolutional Neural Networks (CNN) have
20 proven effectiveness in varied areas; histopathology is not the exception. In [14], a system to support pathologists in cancer diagnosis with improved accuracy, reproducibility and efficiency was developed. In [15], a deep learning method was proposed to address two classification tasks in Hematoxylin- and Eosin-stained tissue images: cancer classification based on immunohistochemistry and
25 necrosis detection regarding necrosis presence extents. In [16], a method to classify glioma and non-small-cell lung carcinoma cases into subtypes was proposed. In [17], a network-based tool was proposed to segment nuclei, epithelium (stroma vs epithelium) and tubule; detect lymphocyte, mitosis and invasive ductal carcinoma; and classify lymphoma. Nevertheless, none of these CNN-based
30 techniques addresses the automatic classification of normal tissues and organs of the human cardiovascular system.

Preliminary advances have been made in identification and classification of organs and fundamental tissues of the cardiovascular system. These methods have been built using image processing techniques, tissue morphological and
35 textural information, and supervised learning. In particular, we have worked on two research lines: segmentation and classification of cells and fibres, allowing recognition of epithelial, loose connective and muscle tissues [18, 11, 19] and classification of fundamental tissues and some organs [1, 2, 3, 20].

In this paper, we present an approach to classify the fundamental tissues
40 and, in some cases, organs of the human cardiovascular system automatically. We use transfer learning on well-known deep CNNs to recognise the cardiac muscle, loose connective tissue (vein, arteries and the heart), smooth muscle of muscular artery, large vein, elastic artery, and light regions. In this way,

we devise a more general and robust method that outperforms our previous
45 works [2, 3] and, at the same time, allows us to recognise organs.

The rest of this paper is structured as follows. The proposed approach for
automatically classifying fundamental tissues and organs is explained in detail
in Section 2. The dataset, experiments and results are described in Section 3.
In Section 4, we analyse the obtained results. Finally, the main conclusions of
50 this work are drawn in Section 5.

2. Method

A fundamental tissue exhibits unique patterns that permit identifying and
differentiating it from others. Likewise, an organ can be recognised by knowing
the tissues present in its histological samples. However, the tissue appearance
55 may vary within the same organ sample preparation (cut and stain processes)
or image acquisition settings (microscope and software). For example, thermal
drift and colour samples are two sources of acquisition-related intra-class het-
erogeneity as they introduce small variations in colour and lightning. Note that
colour is not a reliable feature in histological images as differences in muscular
60 staining may invalidate the results. Fig. 1 shows blocks of 100×100 pixels
extracted from different tissues and light regions. The variability and similarity
among them can be observed.

We apply a transfer learning strategy to adapt four networks trained for
visual object recognition to a different domain, cardiovascular tissue and organ
65 classification. The considered process consists of four main steps which are de-
picted in Fig. 2. 1) Both training and testing images are tiled up into blocks
of 100×100 . At this level, a block is considered if it complies with two con-
straints: it contains only one type of tissue, and it has discriminant information
that makes tissue recognition possible. 2) A network trained for visual object
70 recognition on natural images is updated to process data from our domain us-
ing a transfer learning strategy. We use the weights learnt from ImageNet to
initialise the network, and fine-tune it to recognise cardiovascular tissues and

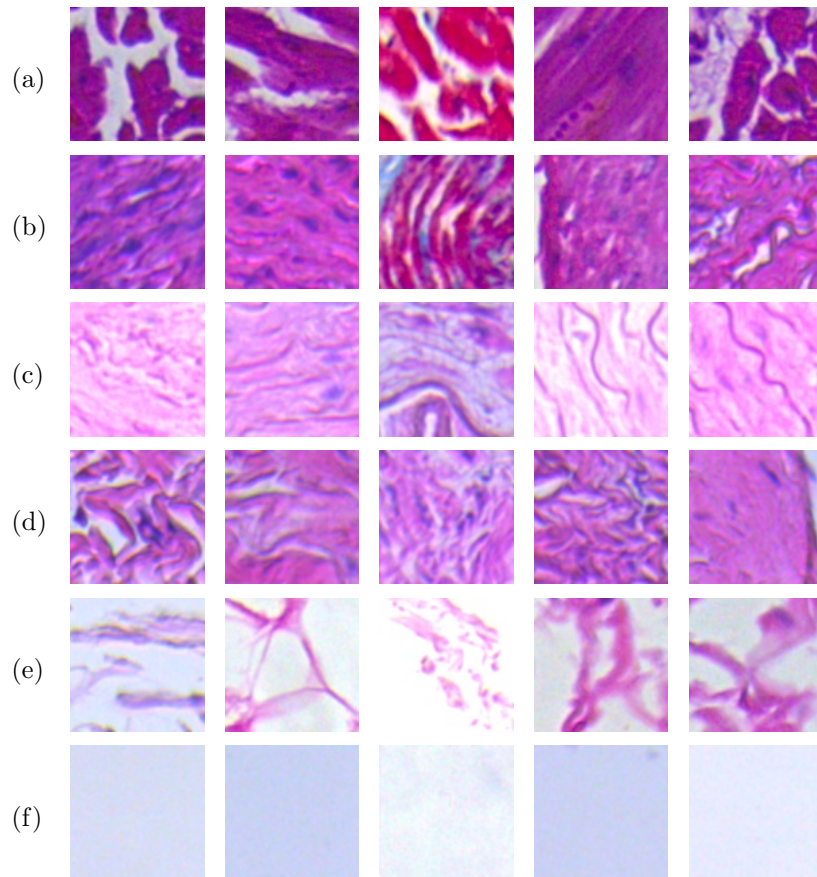


Figure 1: Examples of variability in tissue patterns. From top to bottom, (a) "Heart" symbolises the cardiac muscle, (b) "Muscular" corresponds to the smooth muscle of muscular artery, (c) "Elastic" represents smooth muscle of the elastic artery, (d) "Vein" stands for the smooth muscle of the large vein, (e) "Connective" identifies the loose connective tissue, and (f) "Light" indicates light regions.

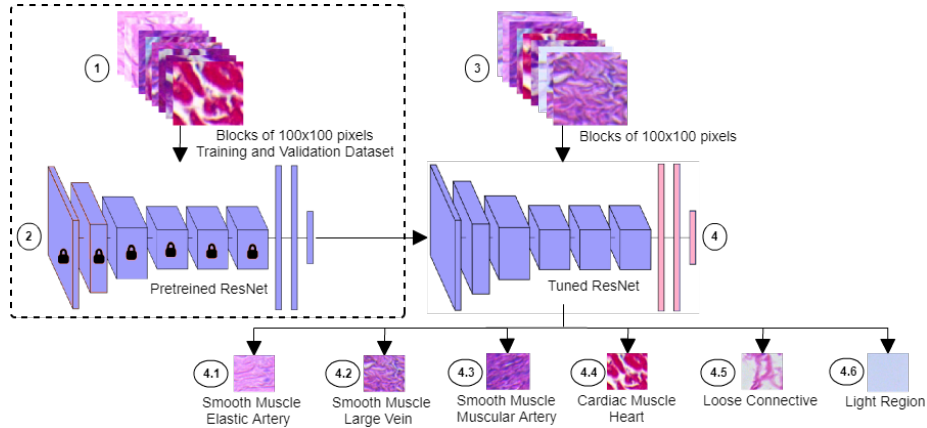


Figure 2: Proposed transfer learning approach for automatic classification of fundamental tissues associated with an organ: (1) image blocks of 100×100 pixels belonging to training and validation dataset. (2) pre-trained network. (3) image blocks of 100×100 pixels. (4) fine-tuned model. (4.1), (4.2), (4.3), (4.4), (4.5) and (4.6) classified blocks.

organs. Note that the domain-specific knowledge is given through the training samples. 3) Blocks of 100×100 pixels from the test set are selected without
75 restrictions. 4) The model resulting from Step 2 is used to classify the content of each one of the blocks into one of the following six classes: 4.1) smooth muscle of the elastic artery; 4.2) smooth muscle of the large vein; 4.3) smooth muscle of the muscular artery; 4.4) cardiac muscle; 4.5) loose connective tissue; 4.6) light regions. The details of the complete process are presented in this section.

80 *2.1. Classification using transfer learning*

A CNN trained for performing a certain task can be adapted to deal with another one. A common transfer learning approach consists of using the convolutional layers as fixed feature extractors and adjusting only the fully connected layers to the new problem. Two of the main benefits as a consequence of freezing the convolutional layers are fast training and the possibility of training deep
85 architectures on small datasets.

In this paper, we adapt four well-known architectures in the state of the art of large-scale visual recognition to the problem of cardiovascular tissue and

Table 1: Details of the different architectures transferred to our domain.

Item	VGG16	VGG19	Inception	ResNet
<u>General</u>				
Parameters	15.5M	20.8M	24.1M	25.9M
Channels	3	3	3	3
Input size	100×100	100×100	150×150	200×200
<u>Number of layers</u>				
Convolutional	13	16	94	53
Max pooling	5	5	4	1
Fully connected	3	3	3	3
<u>Presence of modules</u>				
Batch normalisation	no	no	yes	yes
Residual connections	no	no	no	yes

organ classification. The considered architectures are VGG16 [21], VGG19 [21],
90 Inception [22] and ResNet [23]. These four networks were selected as: (i) they
have achieved top performances in different challenges, (ii) they have inspired
other designs in a variety of research areas – usage of small kernels instead of
large ones, multi-scale architectures and residual connections – and – perhaps
more importantly – (iii) their weights are available to be modified. These pre-
95 trained models are downloaded from the Keras webpage² and loaded onto the
corresponding architecture. The convolutional layers are fixed to avoid any
modification on the training phase, and the fully connected layers are altered
to the new problem by modifying the output vector length to six. Afterwards,
the training phase takes place. More details of the specific implementations are
100 listed in Table 1. For the sake of referring to the resulting fine-tuned models,
we add the prefix *Histo-* to the base name.

²<https://keras.io/applications>

2.2. Crafted ad-hoc architecture

To compare the performance of a network using transfer learning with one trained on the specific scenario from scratch, we design our own architecture and evaluate it under the same conditions. The architecture corresponds to a multi-
105 path design inspired by the work of [24]. As illustrated in Fig. 3, the network is formed by three independent branches, which are later merged to produce the output. The inputs of each path are the RGB channels of the target 25×25 patch. This configuration allows the model to incorporate different sources
110 of information and aggregate various useful features. Hence, it is possible to achieve a consented and more accurate result. Each path consists of three convolutional layers with 24, 32 and 48 kernels, followed by max-pooling layers with stride size of 2×2 . Once the three convolutions take place, the output of the third layer is flattened and input into a dropout layer. This component
115 is placed at this level to prevent the network from memorising the training sample [25, 26]. Then, the resulting vector is used in a fully-connected layer with 256 units. The resulting vectors from the three branches are averaged and, subsequently, connected to the softmax output layer with six nodes. As this last layer returns scores per class, the output class corresponds to the one obtaining
120 the highest response.

2.3. CNN vs Support Vector Machines (SVM)

We consider one of the most used techniques in machine learning, SVM, to contrast with the performance of a network using transfer learning. A cascade SVM based on LBP descriptors presented in [2] is used. This comparison is rel-
125 evant in the histological context since, according to the author’s knowledge, no previous work assesses both techniques for classification of normal fundamental tissues and organs using histological images. On the one hand, a CNN learns features directly from the data and how to use them to produce the expected output. On the other hand, SVM uses carefully engineered features [27] — after
130 performing an extensive analysis of the problem. An exhaustive comparison of different texture descriptors — e.g. Haralick, LBP and LBPri — and classifiers

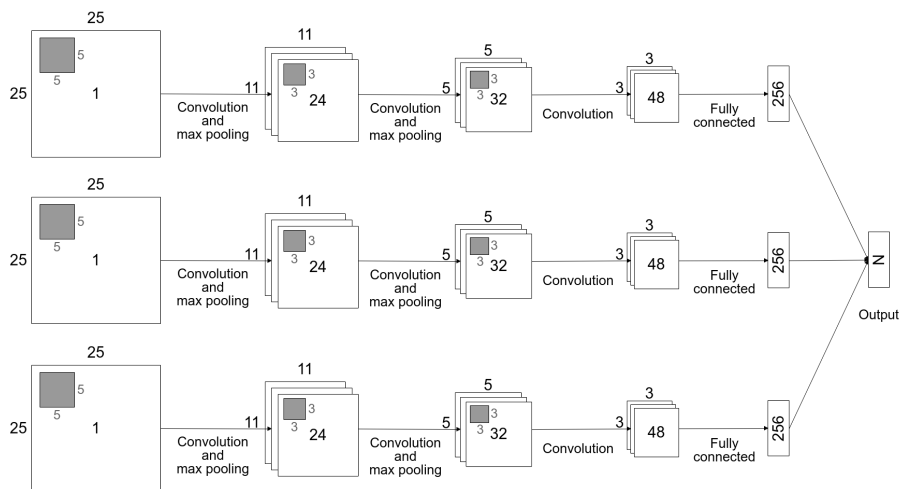


Figure 3: HistoNet architecture inspired by the work in [24]. The network corresponds to a three-path CNN in which each branch takes as input information from one of the RGB channels of the image.

— Random Forest varying initial parameters and classical multi-class SVM using various kernels — was carried out by Mazo *et al.* [2]. From this work, two relevant remarks were drawn. First, among all the evaluated descriptors, the best texture feature to use in this problem is the concatenation of LBP and LBPri. Given a block from a histological image, the LBP+LBPri descriptor is created by concatenating histograms from the LBP ($lbp = [l_1, l_2, \dots, l_{256}]$) and the LBPri ($lbpri = [lr_1, lr_2, \dots, lr_{36}]$) as follows:

$$LBP + LBPri = [lbp||lbpri] = [l_1, l_2, \dots, l_{256}, lr_1, lr_2, \dots, lr_{36}], \quad (1)$$

where $LBP + LBPri$ is a vector of 292 elements. Second, among the evaluated classifiers, a cascade SVM with linear and polynomial kernels yielded the best results. The degree of the polynomial kernel was set to 3 after exhaustive experimentation. Finally, the authors proposed an approach to automatically classify the fundamental tissues and organs of the human cardiovascular system utilising LBP descriptors and a cascade SVM with linear and polynomial kernels to identify six classes: cardiac muscle, smooth muscle of the muscular artery,

Table 2: Labels and corresponding description for each one of the considered classes.

Label	Description
Muscular	Smooth muscle of the muscular artery
Heart	Cardiac muscle
Connective	Loose connective tissue (i.e. veins, arteries and the heart)
Elastic	Smooth muscle of the elastic artery
Vein	Smooth muscle of the large vein
Light	Light regions

loose connective tissue, smooth muscle of the large vein, smooth muscle of the elastic artery, and light regions.

3. Experiments and Results

In this section, we present the complete process that supports the proposed approach. We show the results obtained at three comparison stages: (i) among CNN models obtained through transfer learning, (ii) between HistoResNet and HistoNet and (iii) between HistoResNet and a cascade SVM approach [2]. Three measures based on the confusion matrix are used to assess the response of this work in the classification of the six classes indicated in Table 2: Precision, Recall and F-score. Given the number of true positives (TP), false positives (FP), true negatives (TN) and false negatives (FN), the measures are mathematically expressed as follows:

$$\text{Precision} = \frac{TP}{TP + FP}, \quad (2)$$

$$\text{Recall} = \frac{TP}{TP + FN}, \quad (3)$$

$$\text{F-score} = 2 \cdot \frac{\text{Precision} \cdot \text{Recall}}{\text{Precision} + \text{Recall}}. \quad (4)$$

3.1. Experimental setup

150 **One of the most difficult challenges in this area is to obtain enough annotated samples of normal tissues and organs of the human cardio-**

vascular systems. Although there are public histological datasets, issues that prevent using them are: they were taken from a different species (e.g. mice); they contain pathological samples and not normal ones; they contain a mix of all human systems and not enough samples of the cardiovascular system; and their images were not acquired with standard laboratory and imaging protocols. These and other challenges have been detected and addressed in our previous works [28].

Tissue samples from organs were stained with Hematoxylin and Eosin and Massons trichrome using a laboratory protocol to control the process. The image capture protocol was defined for setting microscope and software configuration, sample manipulation and image capture process to control variability. The histological images were acquired using a Leica *DM750 – M* microscope with a resolution of 2048×1536 pixels and stored in PNG format. The microscope had eyepieces with a magnification factor of $10\times$ and a field of view of 20, obtaining 100 end magnification for a $10\times$ objective.

A dataset of 6000 blocks, 1000 per class, was divided into 70% for training and 30% for validation. Another dataset of 7500 blocks was used for testing and obtaining the results. Images from both datasets were obtained from tissue samples of different organs and persons and acquired at $10\times$ objective. The block size selection is one of the major issues. We used a block size of 100×100 based on the study in [2] which has the following advantages: (i) a fundamental tissue can be recognised and (ii) a large number of blocks contain only one type of tissue. Our ground-truth was provided by the group of six histology experts members of the Teblami research group from the Universidad del Valle³. We have made the datasets at http://biscar.univalle.edu.co/?page_id=1003.

³Grupo de Tejidos Blandos y Mineralizados, Teblami. Research website: <https://sites.google.com/a/correounivalle.edu.co/grupo-de-tejidos-blandos-y-mineralizados>

3.2. Data preparation and training details

As mentioned previously, blocks of 100×100 were extracted from the input
180 images. The values are normalised to obtain zero mean and unit variance per
channel. Note that the mean and standard deviation calculated for the training
set are used later on the test set. Also, since some of the networks require a
specific input size, the blocks were upscaled according to the input sizes shown
in Table 1.

185 The different networks were trained for n epochs on the training set and
assessed on the validation set. After various experiments, we observed that,
in this particular case, the considered networks achieved their best results on
the validation set around the tenth iteration and that there was no notable
improvement afterwards. Hence, we fixed the value of n to 20. The whole
190 training set was passed to the model in mini-batches of 32 elements. To avoid
over-fitting, we forced the training process to stop before iterating n times if no
improvement was observed for more than two iterations. This monitoring was
carried out using early stopping [29].

The deep learning methods were implemented in Python, using the Keras
195 library, and run in a computer with 12 cores, 128Gb RAM and a Geforce GTX
1080 GPU. We have made CNN models publicly available at http://biscar.univalle.edu.co/?page_id=1082.

3.3. CNNs applied to the cardiovascular tissue classification through transfer learning

200 In transfer learning, we compared four of the most used CNNs architectures
for visual object recognition — ResNet, VGG19, VGG16 and Inception. The
obtained Precision and Recall results are presented in Table 3 and Table 4,
respectively. The corresponding F-score values per method and per class are
shown in Fig. 4.

205 HistoVGG networks achieved the highest Precision for Elastic, Muscular,
Heart and Connective with values of 0.963, 0.727, 0.937 and 0.855, respectively.
Nevertheless, HistoResNet obtained the best Precision overall, 0.819. Also,

Table 3: Precision values per class obtained by different CNN architectures using transfer learning

Class	HistoResNet	HistoVGG19	HistoVGG16	HistoInception
Elastic	0.952	0.874	0.963	0.690
Heart	0.902	0.937	0.931	0.918
Muscular	0.712	0.650	0.727	0.579
Connective	0.820	0.855	0.818	0.815
Vein	0.578	0.549	0.434	0.582
Light	0.955	0.928	0.935	0.895
Overall	0.819	0.799	0.801	0.747

Table 4: Recall values per class obtained by different CNN architectures using transfer learning

Class	HistoResNet	HistoVGG19	HistoVGG16	HistoInception
Elastic	0.863	0.886	0.823	0.879
Heart	0.955	0.937	0.939	0.906
Muscular	0.797	0.794	0.737	0.775
Connective	0.772	0.751	0.751	0.660
Vein	0.943	0.809	0.894	0.537
Light	0.829	0.878	0.869	0.863
Overall	0.860	0.843	0.836	0.770

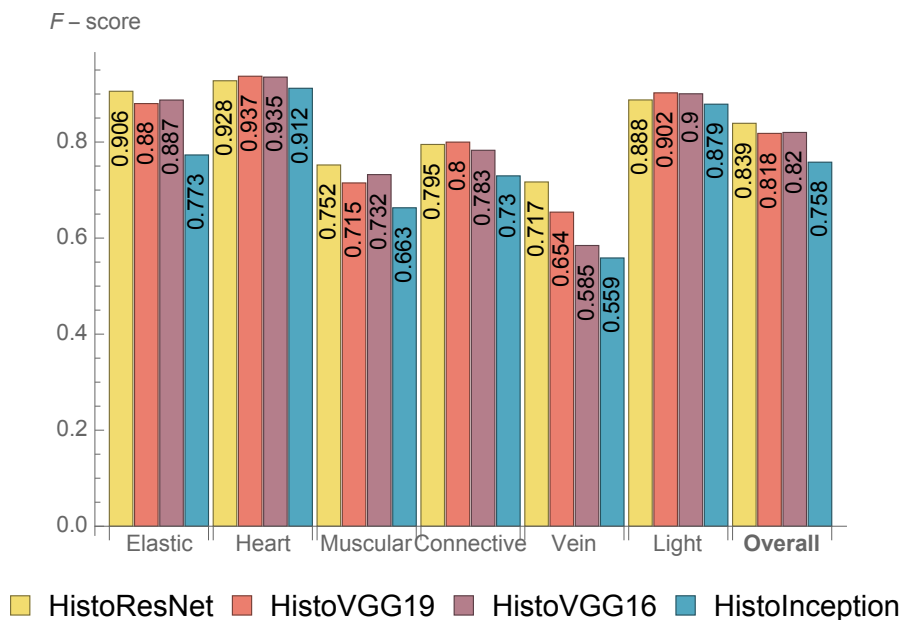


Figure 4: F-score values obtained per class using a transfer learning approach on different CNNs.

the same architecture, HistoResNet, outperformed regarding Recall for Heart, Muscular, Connective, Vein and overall with scores of 0.955, 0.797, 0.772, 0.943 and 0.860, correspondingly.

According to Fig. 4, the topmost results were obtained by HistoResNet for Elastic, Muscular and Vein with an F-score of 0.906, 0.752 and 0.717, respectively. Heart, Connective and Light were better classified using HistoVGG19 with an F-score of 0.937, 0.800 and 0.902, correspondingly. Therefore, overall, the HistoResNet approach outperformed all the other methods with an overall F-score of 0.839. The worst F-score was achieved in the classification of Vein regardless of the considered technique.

3.4. HistoResNet and HistoNet applied to the cardiovascular tissue classification

A new architecture called HistoNet was used to make a comparison between transfer learning and one network trained from scratch on our specific domain. These results are summarised in Table 5 and Fig. 5.

Table 5: Precision and Recall values per class obtained by HistoResNet and HistoNet

Class	Precision		Recall	
	HistoResNet	HistoNet	HistoResNet	HistoNet
Elastic	0.952	0.984	0.863	0.687
Heart	0.902	0.923	0.955	0.898
Muscular	0.712	0.531	0.797	0.802
Connective	0.820	0.779	0.772	0.741
Vein	0.578	0.470	0.943	0.844
Light	0.955	0.929	0.829	0.839
Overall	0.819	0.769	0.860	0.802

The best Precision scores for Muscular, Connective, Vein and Light were 0.712, 0.820, 0.578 and 0.955, respectively, and were obtained using HistoResNet. The highest Precision for Elastic and Heart, 0.984 and 0.923, was achieved using HistoNet. HistoResNet yielded the highest Precision overall, 0.819. Also, HistoResNet obtained the best Recall for Elastic, Heart, Connective and Vein with values of 0.863, 0.955, 0.772 and 0.943, respectively, while HistoNet produced outstanding classification values for Muscular and Light, 0.802 and 0.839. HistoResNet achieved the best Recall overall, 0.860.

Based on the F-score results shown in Fig. 5, HistoResNet outperforms HistoNet regardless of the class. The largest gaps between both methods are observed for Elastic, Muscular and Vein, where the scores of HistoResNet surpass the ones of HistoNet in more than 10%. The smallest gaps are seen for Heart and Light where the difference is less than 2%.

3.5. HistoResNet vs a cascade SVM approach

We compared our HistoResNet against the cascade SVM proposed in [2] using our dataset, the results are summarised in Table 6. The best F-score results were obtained by the CNN proposal for both Precision and Recall, for all the classes and in overall. The highest difference between both methods in Precision is observed for the Muscular class, and regarding Recall, for Vein class.

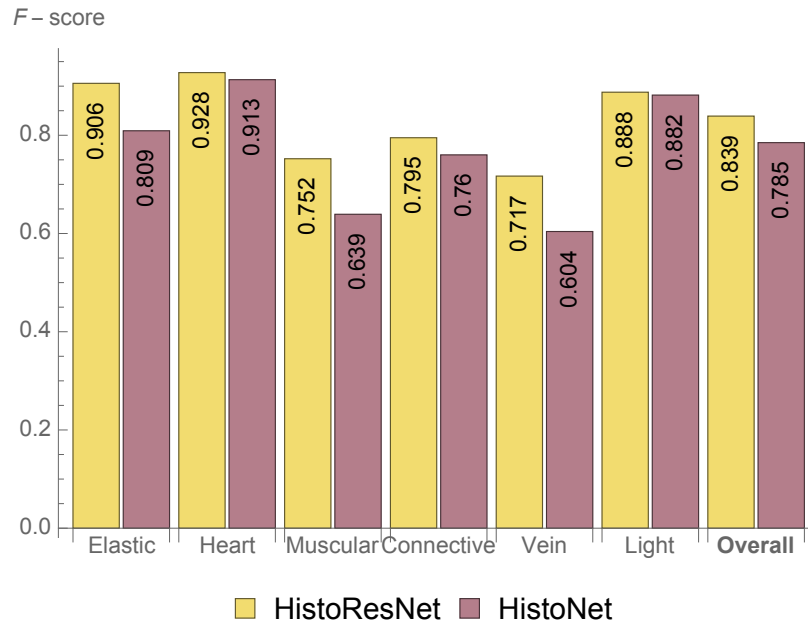


Figure 5: F-score values obtained per class using ResNet vs HistoNet.

Table 6: Precision and Recall values per class obtained by HistoResNet and SVM

Class	Precision		Recall	
	HistoResNet	SVM	HistoResNet	SVM
Elastic	0.952	0.811	0.863	0.622
Heart	0.902	0.848	0.955	0.745
Muscular	0.712	0.442	0.797	0.660
Connective	0.820	0.711	0.772	0.671
Vein	0.578	0.455	0.943	0.568
Light	0.955	0.803	0.829	0.814
Overall	0.819	0.678	0.860	0.680

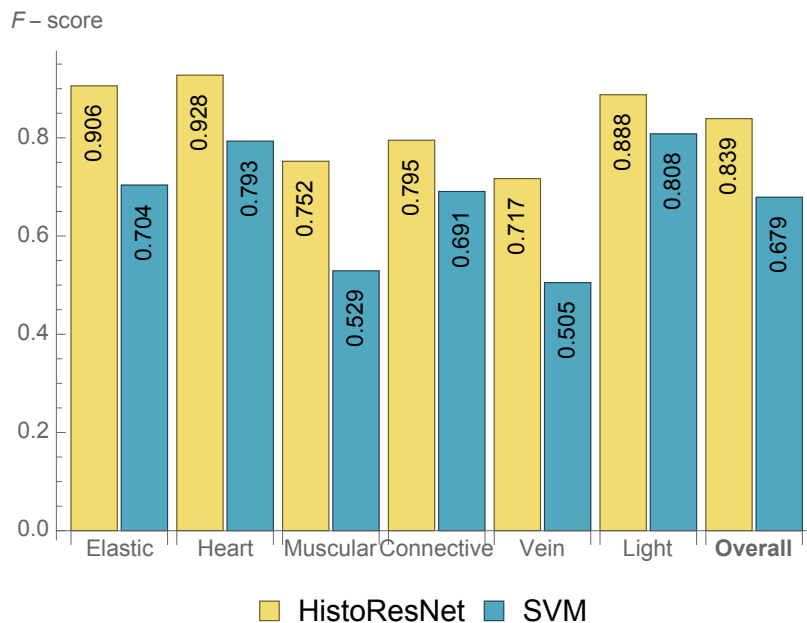


Figure 6: F-score values obtained per class using HistoResNet vs SVM.

The comparison results are illustrated in Fig. 6. The best results were obtained using our HistoResNet for all classes, for all measures. The increase in F-score varies in the range from 8% to 22% compared to the cascade SVM strategy.

245 **4. Discussion**

In the last years, CNNs have been successfully applied to different histopathology problems [14, 15, 16], but due to the usual lack of sufficient annotated data, training these approaches from scratch leads to poor models. This issue can be bypassed by using transfer learning, adjusting a well-trained network on a certain domain to another one. Commonly, convolutional layers are kept as general
 250 feature extractors and only fully connected layers are retrained. Consequently, less data is required for fine-tuning pre-trained networks.

We used transfer learning to adapt four well-trained deep networks to classify normal cardiovascular tissues and to recognise organs. The fine-tuned models

255 were evaluated at three stages. Firstly, we compared their results to determine
which one was the best classifier. We observed that HistoResNet, our modified
ResNet architecture, achieved the best overall performance. Secondly, we con-
trasted our approach against HistoNet, our ad-hoc 2D multi-path CNN, finding
out that, in general, the latter approach performed worse. From our point of
260 view, this outcome suggests that the networks obtained through transfer learn-
ing are not necessarily in disadvantage to the ones entirely trained on the specific
domain. Thirdly, we assessed our proposal against the state of the art, an ap-
proach based on a cascade SVM presented in [2]. The obtained results showed
that our method outperforms the SVM one in terms of Precision, Recall and F-
265 score, regardless of the classes considered. Our proposal obtains improvements
in F-score of 0.159 ± 0.061 , achieving the best accuracy up to date.

Two trends were observed regarding the classification of the six classes. On
the one hand, Vein exhibited the least Precision and F-score compared to the rest
of the classes, what can be due to the similarity between both types of tissues.
270 It is important to highlight that this situation is not limited to our classification
algorithms as it was already observed during the manual annotations as well.
On the other hand, Heart was consistently the best-classified class in terms of
F-score.

5. Conclusions

275 In this paper, we presented an application of transfer learning to classify
normal cardiovascular tissues and organs from histological images. Four well-
known CNNs architectures trained to recognise visual objects on natural images
(in particular, ResNet, VGG16, VGG19, Inception) were fitted to this problem.
Our transfer learning strategy consisted of keeping and freezing the convolu-
280 tional layers and updating the fully connected layers to the new scenario. The
initial weights of the networks were the ones obtained on their previous training
on the ImageNet dataset. The prefix Histo- was used to denote the resulting
models.

Training deep CNN models requires a massive amount of data. Although
285 our training set does not contain as many images as ImageNet and we did not
use data augmentation, the four networks produced high F-scores for most of
the classes. This outcome highlights the main virtue of transfer learning, its
ability to use the potential of deep learning on domains with a reduced number
of training samples. Our proposal was evaluated at three levels. Initially, the
290 four adapted networks were compared with each other. We determined that the
best CNN using the transfer learning strategy was HistoResNet, which yielded
F-score between 0.712 and 0.955. Then, the leading CNN was compared against
a network trained solely on our training set, called HistoNet. We concluded that
HistoResNet was better than HistoNet. This situation showed that it is not nec-
295 essary to train networks from scratch to achieve top results as pre-trained models
can be adapted to different domains without compromising performance. The
classification scores of both strategies exhibited similar trends. Afterwards, our
deep learning method was compared against a traditional machine learning ap-
proach, a cascade SVM approach using LPB descriptors. Our proposal achieved
300 improvements in F-score between 0.080 and 0.220 in comparison to the state of
the art.

The outcome of this research is five-fold. First, we found out that it is possible
to classify normal cardiovascular tissues automatically using deep learning
and transfer learning. Second, we showed that it is feasible to recognise several
305 cardiovascular organs through the same process. Third, we made our training
and test set, both models and source code, publicly available. In this way, the
community can understand our proposal in depth, use the methods and datasets
as a benchmark, validate our results and work in further improvements. Fourth,
we created an ad-hoc 2D multi-path network specially crafted for our problem
310 which yielded an average F-score of 0.768. And finally, we can conclude by
saying that CNNs are very suitable to improve tissue and organs classification.

In the future, we will extend this proposal by working in the following three
research lines. Firstly, we plan to expand the application spectrum by consid-
ering other human systems. Secondly, we want to include histological ontolo-

315 gies [30], morphological information and SPARQL queries. This will allow us
to correct misclassified image blocks and include histological information di-
rectly into the process (see a first attempt in [20]). Thirdly, Thirdly, we are
planning to integrate the proposed method as additional functionality to the
“*Banco de Imágenes Histológicas del Sistema Cardiovascular*” (BISCAR) [28],
320 publicly available at <http://biscar.univalle.edu.co>.

6. Acknowledgements

This work has been supported by COLCIENCIAS and Asociación Univer-
sitaria Iberoamericana de Postgrado, AUIP. Claudia Mazo holds a grant from
the EI and from the European Union’s Horizon 2020 research and innovation
325 programme under the Marie Skłodowska-Curie grant agreement No 713654. Jose
Bernal holds an FI-DGR2017 grant from the Catalan Government with refer-
ence number 2017FI B00476. We thank Liliana Salazar, MSc., for providing
insight and expertise that greatly assisted the research.

References

- 330 [1] C. Mazo, M. Trujillo, E. Alegre, L. Salazar, Automatic recognition of fun-
damental tissues on histology images of the human cardiovascular system,
Micron 89, 2016, 1–8.
- [2] C. Mazo, E. Alegre, M. Trujillo, Classification of cardiovascular tissues
using LBP based descriptors and a cascade SVM, Computer Methods and
335 Programs in Biomedicine 147, 2017, 1–10.
- [3] C. Mazo, E. Alegre, M. Trujillo, V. González-Castro, Tissues Classification
of the Cardiovascular System Using Texture Descriptors, in: Annual Con-
ference on Medical Image Understanding and Analysis, Vol. 723, Springer,
2017, 123–132.
- 340 [4] I. Masic, E-learning as new method of medical education, Acta informática
médica 16 (2), 2008, 102–117.

- [5] J. Ruiz, M. Mintzer, R. Leipzig, The Impact of E-Learning in Medical Education, *Academic Medicine* 81 (3), 2006, 207–212.
- [6] A. I. Hernández, S. M. Porta, M. Miralles, B. F. García, F. Bolúmar, La cuantificación de la variabilidad en las observaciones clínicas, *Med Clin*, 345 1990, 424–429.
- [7] N. Hervé, A. Servais, E. Thervet, J. C. Olivo-Marin, V. Meas-Yedid, Statistical color texture descriptors for histological images analysis, in: 2011 IEEE International Symposium on Biomedical Imaging: From Nano to Macro, IEEE, 350 2011, 724–727.
- [8] E. González-Rufino, P. Carrión, E. Cernadas, M. Fernández-Delgado, R. Domáñez-Petit, Exhaustive comparison of colour texture features and classification methods to discriminate cells categories in histological images of fish ovary, *Pattern Recognition* 46 (9), 2013, 2391–2407.
- [9] A. D. Belsare, M. M. Mushrif, M. A. Pangarkar, N. Meshram, Classification of breast cancer histopathology images using texture feature analysis, in: TENCON 2015 - 2015 IEEE Region 10 Conference, IEEE, 2015, 1–5.
- [10] A. Anuranjeeta, K. Shukla, A. Tiwari, S. Sharma, Classification of Histopathological images of Breast Cancerous and Non Cancerous Cells Based on Morphological features, *Biomed Pharmacol* 10, 2017, 353–366. 360
- [11] C. Mazo, M. Trujillo, L. Salazar, Automatic classification of coating epithelial tissue, in: Iberoamerican Congress on Pattern Recognition, Springer, 2014, 311–318.
- [12] L. He, L. R. Long, S. Antani, G. R. Thoma, Histology Image Analysis for Carcinoma Detection and Grading, *Comput. Methods Prog. Biomed.* 365 107 (3), 2012, 538–556.
- [13] M. Aswathy, M. Jagannath, Detection of breast cancer on digital histopathology images: Present status and future possibilities, *Informat-ics in Medicine Unlocked* 8 (Supplement C), 2017, 74–79.

- 370 [14] N. Hatipoglu, G. Bilgin, Classification of histopathological images using convolutional neural network, in: 2014 4th International Conference on Image Processing Theory, Tools and Applications (IPTA), 2014, 1–6.
- [15] H. Sharma, N. Zerbe, I. Klempert, O. Hellwich, P. Hufnagl, Deep convolutional neural networks for histological image analysis in gastric carcinoma whole slide images, *Diagnostic Pathology* 1 (8), 2016, 1–3.
- 375 [16] L. Hou, D. Samaras, T. M. Kurç, Y. Gao, J. E. Davis, J. H. Saltz, Efficient Multiple Instance Convolutional Neural Networks for Gigapixel Resolution Image Classification, *CoRR* abs/1504.07947, 2015, 1–9.
- [17] A. Janowczyk, A. Madabhushi, Deep learning for digital pathology image analysis: A comprehensive tutorial with selected use cases, *Journal of Pathology Informatics* 7 (1), 2016, 29–47.
- 380 [18] C. Mazo, M. Trujillo, L. Salazar, An automatic segmentation approach of epithelial cells nuclei, in: *Iberoamerican Congress on Pattern Recognition*, Springer, 2012, 567–574.
- [19] C. Mazo, M. Trujillo, L. Salazar, Identifying loose connective and muscle tissues on histology images, in: *Iberoamerican Congress on Pattern Recognition*, Springer, 2013, 174–180.
- 385 [20] C. Mazo, M. P. Trujillo, E. Alegre, L. Salazar, Ontology-based automatic reclassification of tissues and organs in histological images, in: *Proceedings of the 12th Alberto Mendelzon International Workshop on Foundations of Data Management*, 2018, 1–4.
- 390 [21] K. Simonyan, A. Zisserman, Very Deep Convolutional Networks for Large-Scale Image Recognition, *CoRR* abs/1409.1556, 2014, 1–14.
- [22] C. Szegedy, W. Liu, Y. Jia, P. Sermanet, S. Reed, D. Anguelov, D. Erhan, V. Vanhoucke, A. Rabinovich, Going deeper with convolutions, in: *Proceedings of the IEEE conference on computer vision and pattern recognition*, 2015, 1–9.
- 395

- [23] K. He, X. Zhang, S. Ren, J. Sun, Deep residual learning for image recognition, in: Proceedings of the IEEE conference on computer vision and pattern recognition, 2016, 770–778.
- 400 [24] P. Moeskops, M. A. Viergever, A. M. Mendrik, L. S. de Vries, M. J. Benders, I. Išgum, Automatic segmentation of MR brain images with a convolutional neural network, IEEE transactions on medical imaging 35 (5), 2016, 1252–1261.
- 405 [25] S. Wager, S. Wang, P. S. Liang, Dropout training as adaptive regularization, in: Advances in neural information processing systems, 2013, 351–359.
- [26] N. Srivastava, G. Hinton, A. Krizhevsky, I. Sutskever, R. Salakhutdinov, Dropout: A Simple Way to Prevent Neural Networks from Overfitting, Journal of Machine Learning Research 15, 2014, 1929–1958.
- 410 [27] Y. LeCun, Y. Bengio, G. Hinton, Deep learning, Nature 521 (7553), 2015, 436–444.
- [28] M. Santamaria, Y. Muñoz, E. Cuellar, C. Mazo, S. Scotti, L. Salazar, M. Trujillo, BISCAR: Banco de Imágenes Histológicas del Sistema Cardiovascular, Vol. 2015, 2014, 104–105.
- 415 [29] I. Goodfellow, Y. Bengio, A. Courville, Deep Learning, MIT Press, 2016.
- [30] C. Mazo, L. Salazar, O. Corcho, M. Trujillo, E. Alegre, A histological ontology of the human cardiovascular system, Journal of biomedical semantics 8 (1), 2017, 47–62.